Research article

Investigation of clay brick waste for the removal of copper, nickel and iron from aqueous solution: batch and fixed – bed column studies

Gobusaone Mokokwe [a,b], Moatlhodi Wise Letshwenyo [a,b,*]

[a] Botswana International University of Science and Technology, Faculty of Engineering and Technology, Botswana
[b] Department of Civil and Environmental Engineering, Private Bag 16, Palapye, Botswana

ABSTRACT

The adsorption of copper, iron and nickel ions from an aqueous solution using Makoro granite clay brick waste through batch and fixed – bed column modes was investigated. The adsorbent was characterised using X-Ray Fluorescence, X-Ray Diffraction (XRD), Thermogravimetric Analysis, and Scanning Electron Microscopy (SEM). XRD results revealed crystalline peaks of Quartz (51.28 %) and mullite (23.40%) in fresh and loaded adsorbent with unnotable changes before and after adsorption. SEM images indicate the presence of micro pores and irregularly distributed surfaces. Batch kinetic maximum adsorption capacities for iron, copper, and nickel are 7.60, 6.70 and 6.20 mg g^{-1} media respectively with 60 min as the optimum time. The maximum adsorption capacities at adsorbent dosage of 5 g L^{-1} were 10.0, 7.60 and 7.20 mg L^{-1} for iron, copper and nickel ions. The corresponding adsorption capabilities from the fixed-bed column reactor were 2.23, 2.22 and 0.74 mg g^{-1} media respectively. The thermodynamics parameters of enthalpy change (ΔH) were 5.21, 9.32 and 5.22 kJ mol^{-1} respectively for Copper, iron and nickel ions and the corresponding entropy change (ΔS) were -0.04, -0.05 and -0.03 kJmol^{-1}K^{-1} respectively and the process being non-spontaneous and exothermic. Thomas and Yoon-Nelson models yielded similar low coefficient of determination (R^2) values (0.06 and 0.07) for copper and iron ions. Further investigations such as the use of real wastewater, competition of anions and further media characterisation and modifications are recommended.

1. Introduction

Because of water shortage, wastewater treatment systems are being upgraded to produce effluent of high quality which can be reused for other needs (Foroutan et al., 2020). The contamination of aquatic systems by heavy metals is of global concern world-wide and therefore need of efficient technology for their removal (Wołowiec et al., 2019). Globally, water demand, and water scarcity are likely to be exacerbated in the future as a result of rapid industrialization, burgeoning population and urbanisation. The development of industries contributes to this challenge of wastewater characterised by laden heavy metals (Younas et al., 2021). There is a need to pay special attention to heavy metals due to their toxic, mutagenic, carcinogenic, teratogenicity characteristics (Farooq et al., 2010).

The discharge of industrial effluent with heavy metals into aquatic environments in excess of threshold limits has increased (Iloms et al., 2020). Despite their toxic, carcinogenic, mutagenic and teratogenic behaviour, heavy metals are required by human systems in small quantities to perform some vital functions (Ali et al., 2019). In addition, these effluents contain nutritious organic compounds that improve the fertility of agricultural soils (Usman et al., 2012). The challenge of water pollution has impeded aspirations for the achievement of 2030 Sustainable Development Goal (SDG); clean water and sanitation (Omopariola and Adeniyi, 2021).

To overcome the situation of aquatic pollution by heavy metals, regulatory bodies such as the European Union (EU), the World Health Organisation (WHO), and locally the Botswana Bureau of Standards (BOBS) have set strict water quality standards (Vareda et al., 2019). To date, many developing countries are faced with water shortages and instead use treated wastewater to irrigate crops. The wastewaters are not properly treated and can cause various illnesses in human and peripheral ecosystems (Neris et al., 2019; Duan and Fedler, 2021). Some vegetables such as spinach have shown the ability to accumulate heavy metals in various edible parts (Letshwenyo and Mokokwe, 2020). To overcome the toxicological illnesses that people who eat food contaminated with heavy metals are exposed to, the Food and Agriculture Organisation (FAO) and

---

the United States Environmental Protection Agency (USEPA) have enacted stringent laws for limiting the concentrations of heavy metals in wastewater (Babel and Kurniawan, 2003). Nickel, copper and iron are some of the heavy metals mostly found in high concentrations in industrial effluents and even in the surface waters (Njoku et al., 2020).

Due to their toxicity, organisations such as the World Health Organisation (WHO) have set permissible limits for heavy metals in aqueous environments. These consents serve to protect the environment and human life, including aquatic and abiotic life (Table 1).

According to Amuda et al. (2006), numerous traditional wastewater treatment techniques such as flocculation and coagulation have been used to reduce toxic heavy metal ions from wastewater. In addition, studies have been conducted on other treatment techniques such as ion exchange (Tan et al., 2017), chemical precipitation (Ramakrishnaiah and Prathima, 2016; Brbooti et al., 2011), photo-catalysis (Ku and Jung, 2001), reverse osmosis (Thaçi and Gashi, 2019), membrane filtration (Khulbe and Matsuura, 2018). Among these technologies, chemical precipitation has been the most widely used technique for reducing heavy metal ions from wastewater. The challenges that i researchers experience during the application of chemical precipitation are the generation of bulky sludge and the need to use large storage infrastructures, which make the process unfavourable (Manjuladevi et al., 2018). On the other hand, Zhang and Wang (2015) reported that adsorption is a cost effective, feasible, and effective technology that can be used to remove toxic heavy metal ions in contaminated water. Ion exchange is one of the processes that has been used to remove heavy metals from aqueous solutions or wastewaters.

Below are the disadvantages of the conventional technologies that have been used previously (Table 2).

According to Duan and Fedler (2021), many scientists have focused on the use of feasible and abundant adsorbents in the adsorptive removal of contaminants, including heavy metals from effluents. To date, studies are more dedicated to implementation of contaminant removal utilizing waste materials (Visa, 2016). Some of the less costly waste materials such as coal fly ash, silicate tailings, coal clinker and many others have been studied in adsorption (Table 3). There are limited studies on heavy metal removal using brick waste. El-Shahat and Shehata (2013) investigated the adsorption of lead, cadmium and zinc from wastewater using clay brick, and found that the adsorption process was effective. Local construction companies have generated piles of solid waste, including brick waste. The use of clay brick waste also poses environmental management concerns for waste disposal in large quantities, resulting in air, soil and water pollution. Research on adsorptive removal of heavy metals from effluents using construction waste is limited in Botswana. In the manufacturing process of bricks at Makoro, the clay is mixed with coal fines from the Morupule coal mine and subjected to high temperatures of around 1350 °C. The activation or heat treatment of clay and mixing it with coal may improve the adsorptive properties of the material. There is no study on the adsorption of heavy metals using Makoro clay brick has in Botswana. Therefore, it is very important to close this gap in the study of adsorption of metal ions using construction waste materials.

Table 1. Permissible limits for potable water of some heavy metals (mgL^{-1}) (Ahmaruzzaman, 2011).

Metals	WHO	USEPA	EU
Nickel	0.02	0.1	0.02
Zinc	3.0	5.0	-
Copper	2.0	1.3	2.0
Cadmium	0.003	0.005	0.005
Lead	0.01	0.015	0.01
Arsenic	0.01	0.01	0.01
Mercury	0.001	0.002	0.001
Iron	0.2	0.3	0.2
Manganese	0.5	0.05	0.05

Table 2. Disadvantages of the conventional technologies for heavy metals removal from wastewater source (Siong et al., 2021).

Technology	Disadvantages
Ion exchange	• Large volume of water requiring large columns • Fouling by organic matter • Pretreatment required • Sensitive to effluent pH • Selective resins have limited commercial use
Chemical precipitation	• Large volume of sludge produced, hence handling, transport and disposal costs • Low efficiency in removing low concentration metal ions • Oxidation step required if metals are complexed
Membrane filtration	• High energy requirements • High operation and maintenance costs • Rapid fouling on membrane • Limited low rates
Coagulation/flocculation	• Poor removal of arsenic • Large volume of sludge generated
Adsorption	• Methods are non-selective • High cost of materials such as activated carbon • Several types of adsorbents required • Regeneration is expensive

Table 3. Reported performance of some heavy metal adsorbents.

Heavy metal ions	Adsorbent	Initial ionic concentration (mgL^{-1})	Maximum sorption capacity ($mg\,g^{-1}$)	Mode of test	References
Ni^{2+}	Coal fly ash	500	5.00	Batch and fixed – Column bed	(Lekgoba et al., 2020)
Cu^{2+}			11.65		
Cd^{2+}	Synthesised silicate tailings	20–1000	35.36	Batch and fixed – bed Column	(Ouyang et al., 2019)
Cu^{2+}			32.26		
Cu^{2+}	Red soil	10–50	-	Batch	(Mishra et al., 2017)
Ni^{2+}	Black soil	10	-		

Materials or adsorbents such as biochar have been investigated for the removal of heavy metals from wastewater, but it was observed that event though it is an excellent adsorbent, it was difficult to reuse after adsorption for the treatment of wastewater (Son et al., 2018). As a result, the authors developed magnetic biochar through pyrolysis of macro algae and iron oxide particles to improve the quality of the material, and it was observed to be more efficient compared to the other biochar adsorbents. The magnetization of biochar aimed to improve its alit such as limitation in separation and limited ability to remove heavy metals (Liu et al., 2022). Similarly, a magnetic biogas residue-based biochar was prepared and its adsorption capacities for the removal of copper and lead ions from wastewater were 75.76 and 181.82 mgg^{-1} media, respectively, indicating high efficiency as Pan et al. (2020) reported.

The objective of this work was to investigate the feasibility of using clay brick waste as an adsorbent for the removal of divalent Iron (Fe^{2+}), nickel (Ni^{2+}) and copper (Cu^{2+}) ions from aqueous solutions. In doing so, adsorptive removal of divalent Fe^{2+}, Ni^{2+} and Cu^{2+} from multicomponent solution utilising clay brick waste was evaluated in batch and fixed – bed column modes. To obtain the insights on batch and fixed – bed column adsorption mechanisms involved, media was characterised and kinetics, isotherm and fixed - bed column studies conducted. Many previous studies have only conducted batch studies and excluded fixed - bed column (pilot) studies where the results during field trials have proven unrealistic. The use of fixed - bed column reactors at pilot scale is

advantageous over batch reactors because large quantities of wastewater containing different competing ions are treated. In addition, the research using both batch and fixed – bed column modes simultaneously mimics field conditions where the design of the system is much easier than relying on batch results, which are sometimes misleading. During Makoro clay brick manufacturing, clay is mixed with coal fines from Morupule coal mine and exposed to high temperatures of around 1350 °C. The activation or heat treatment of clay and blending with coal may improve the adsorptive properties of the material. No study on adsorption of heavy metals utilising Makoro clay brick has been documented in Botswana.

2. Materials and methods

2.1. Study area

The study was conducted at Botswana International University of Science and Technology (BIUST), Palapye, Botswana. Palapye town is located between the two cities; Gaborone and Francistown at longitude 2708′00′′, latitudes 2233′00′′, 919 m elevation.

2.2. Source and preparation of adsorbent

The samples of clay brick waste by the name Makoro Granite Brick Waste (MGBW) were randomly collected from waste heaps of a clay brick manufacturing company. The samples were mixed to produce a representative sample of a brick waste produced at Makoro (PTY) Ltd. The samples were washed with deionised water (DI) to remove soluble organic materials and other impurities. The sample was air dried after washing and ground using a jaw crusher into smaller particles to be used in characterisation and column adsorption experiment.

2.3. Chemical reagents

A simulated industrial effluent was prepared to replicate ionic concentrations of divalent copper, nickel and iron usually found in effluents of metal refinery works. Stock solutions were prepared using hydrated salts; nickel sulphate ($NiSO_4.6H_2O$) of 99% purity, ferrous sulphate ($FeSO_4.7H_2O$) of 99% purity and copper sulphate ($CuSO_4.5H_2O$) of purity 99.5% distributed respectively by Glass World, Minema and Rochelle Chemicals. Chemicals used for sample preservation (hydrolysis control) and pH adjustment were 65% Nitric acid and sodium hydroxide (NaOH) solutions, both supplied by Sigma-Aldrich.

2.4. Analytical equipment

The fresh and loaded adsorbent was pulverised and characterised by applying X-Ray (XRD), diffractometer (Brucker D8 advance), X-Ray Fluorescence (XRF), (Delta Professional), Scanning Electron Microscopy (SEM), (Carl Zeiss FEGSEM Gemini 500) respectively to find the mineralogical, elemental composition and morphology of the adsorbent. The ionic concentrations of adsorbates and filtrates were measured using calibrated Inductively Coupled Plasma-Optical Emission Spectrometry (iCAP 7000SERIES). Agitation of the adsorbent and solutions was achieved using an Orbital shaker (Thermo Scientific, supplied by Lamworld Technologies Pty Ltd). Thermogravimetric analysis (TGA) was used to evaluate the mass loss and thermal stability of the adsorbent using TGA/DSC3+,manufactured by Mettler Toledo,2018. The functional groups present in MGBW before and after adsorption of heavy metals were determined using a Fourier Transform Infrared Spectrometer (FTIR) (Vertex 70V model), manufactured and supplied by Bruker GmbH in the year 2018.

2.5. Characterisation of the adsorbent

2.5.1. Determination of media pH

The pH of adsorbent was determined in accordance with ASTM D4972 -95A standard operating procedures, as per the procedure of soil pH determination adopted from (US EPA, 2002). The pH meter (Multi-Parameter PCS Testr™ 35) was initially calibrated using pH buffer solutions; pH4.00, pH7.00 and pH10.00. Fresh media was air dried at room temperatures (25 °C). Media sample was sieved through a NO.10 sieve (2.00 mm mesh) to remove coarse fractions. Approximately 10 g of sieved, air-dried media sample was weighed and mixed with 10mL deionised water. The mixture was thoroughly shaken and allowed to stand for about 1 h. The probes were blot dried and the electrode was placed in a partially settled media sample suspensions. Readings were recorded once meter readings had stabilised.

2.5.2. Ionic leaching and pH point of zero charge (pHpzc)

The leachability of the adsorbent was tested using distilled water at pH 6.8 as per Lekgoba et al. (2020). In this study, the agitation times were 24, 48 and 72 h and the analysis of the filtrates was done using ICP-OES. For the pH_{pzc} of the clay brick waste, 0.01 M sodium chloride (NaCl) solution adjusted from pH 2 to pH 10. The 0.5M hydrochloric acid (HCl) solution and the 0.5M sodium Hydroxide solution (NaOH) were used for pH adjustment and the mass of media used was 0.2g, adopted from Hajira et al. (2018).

2.6. Preparation of multiple-element solution

The hydrated sulphate salts (NiSO4.6H2O, CuSO4.5H2O and FeSO4.7H2O) with masses of 4.4840g, 3.9060g and 4.9750g, respectively, were dissolved with double distilled water to prepare 1000ppm multiple stock solutions. Lower ionic concentrations of stock solution were made by dissolving 1000ppm stock solution with distilled water. The stock solution was prepared to mimic the target heavy metal ions, divalent nickel, copper and iron.

2.7. Batch adsorption experiments

In order to investigate the effects of variables such as solution pH, media dose, contact time, temperature, initial concentration and media size, batch adsorption experiments were done. Batch experiments were performed by agitating each adsorbent at 120 rpm in 100 mL aliquot of 200 mg L^{-1} Cu^{2+}, Ni^{2+} and Fe^{2+} at temperatures 293,303, and 313K. The experimental conditions were adsorbent sizes between 0.6mm to 4.75 mm, pH from 2 to 12 and adsorbent dosage from 0.5 to 6.0 g. After 90 min, the solutions were filtered through a 0.45μm filter paper. The filtrates were analysed using ICP – OES (iCAP 7000SERIES) to measure the concentration of target heavy metal ions. The target heavy metal ion removal (%) was computed using Eq. (1) as per Lekgoba et al. (2020).

$$\% = \left(\frac{C_i - C_e}{C_i} \right) \times 100 \tag{1}$$

Where, C_i denotes initial concentration and C_e equilibrium metal concentrations (mg L^{-1}). The uptake capacity of media at time (q_t) was computed using Eq. (2) as per Lekgoba et al. (2020).

$$q_t = \frac{(C_i - C_e)\ V}{M} \tag{2}$$

Where, q_t (mg g^{-1}) denotes heavy metal adsorption capacity of the adsorbent at time, t, M (g) symbolises the MGBW dosage, and V represents the solution volume in (L).

2.7.1. Adsorption kinetic studies

The nature of the reactions taking place during adsorption was explained through batch kinetic modelling. The Lagergren pseudo first order (PFO), pseudo second order (PSO) and Weber-Morris intra-particle diffusion kinetic models were used to identify and describe the rate controlling mechanisms as per Sabela et al. (2019).

2.7.2. Fitness of kinetic models

The Root Mean Square Error (RMSE) analysis along with a coefficient of determination (R^2) was employed to select the suitable kinetic of the adsorption process. RMSE was expressed as descried by Lekgoba et al. (2020) according to Eq. (3).

$$RMSE = \sum \left(\frac{qe, \exp - qe, model}{qe, model} \right)^2 \tag{3}$$

2.7.3. Adsorption isotherm model

The adsorption equilibrium study was conducted at different Cu^{2+}, Fe^{2+} and Ni^{2+} concentrations; 5.0, 10, 25, 50,100 and 200 mgL^{-1} at temperatures of 293K, 303 and 313K. The linearized form of Langmuir isotherm describing sorption was represented by (4) descried by Sabela et al. (2019).

$$\frac{1}{qe} = \frac{1}{qmax} + \frac{1}{qmaxkL} \frac{1}{Ce} \tag{4}$$

Where qe denotes the equilibrium adsorption capacity (mg g^{-1}), Q max (mg g^{-1}) represents the monolayer sorption capacity of the MGBW, *Ce* represents the equilibrium ionic concentration of adsorbates (mg L^{-1}) and K_L denotes Langmuir sorption constant which relates to the free sorption energy (L mg^{-1}) (Sabela et al., 2019). The theoretical assumption of Langmuir isotherm is that adsorption occurs in homogenous active sites.

The Freundlich isotherm model was also employed in the sorption studies to model multilayer sorption of Fe^{2+}, Cu^{2+} and Ni^{2+} on heterogeneous surfaces of adsorbent. The isotherm Eq. (5) takes the linearized form described by Sabela et al. (2019).

$$\log qe = \log Kf + \frac{1}{n} \log Ce \tag{5}$$

where K_f (mg g^{-1}) denotes Freundlich constant relating to sorption capacity, 1/n denotes sorption intensity computed from the slope and the intercept (Flouty and Estephane, 2012).

2.7.4. Thermodynamic studies

Thermodynamic parameters such as Gibbs free energy (ΔG^o, J.mol^{-1}), entropy (DSO, J. molK^{-1}) and enthalpy (ΔH^o, J.mol^{-1}) were used to describe the thermodynamic behaviour of adsorbent. The thermodynamic parameters were computed using mathematical Eqs. (6), (7), and (8) as per Duan and Fedler (2021):

$$\Delta G^0 = -RT\ln kd \tag{6}$$

$$kd = \frac{Ci - Ce}{Ce} x \frac{V}{m} \tag{7}$$

$$\ln kd = \frac{\Delta S^0}{R} - \frac{\Delta H^0}{RT} \tag{8}$$

where kd (Lg^{-1}) denotes the distribution coefficient, T (K) represents the absolute temperature while R (J.molK^{-1}) shows a universal gas constant.

2.8. Column studies

The column set up previously used by Letina and Letshwenyo (2018) was used in this study. However, the experimental column was modified by introducing pumping instead of gravitational flow (Figure 1). Using a pump instead of gravitational flow was more accurate than gravitational flow because a low rate could be easily adjusted compared to adjustment using a control valve, which was difficult and imprecise. In addition, the set up was modified by introducing a rotameter (TECH FLUID) in an influent pipe to adjust the volumetric flow rate. The mass of adsorbent loaded into the column was 10.19 kg with a media size of 4.75, which occupied a bed height of 29 cm, which was a bed volume (BV) of 0.01m^3. The filter bed was fed with a multiple element aqueous solution of initial ionic concentration of 200 ppm through pumping at volumetric flow rate equivalent to 20 mLmin^{-1}. The filtrate was sampled every 90 min and filtered through a 0.45μm filter paper. The samples were preserved as per Haile and Fuerhacker (2018) and ICP-OES was used to measure the target heavy metal concentrations in the filtrates. The adsorption capacity at breakthrough (q$_B$) of clay brick adsorbent was calculated in mg g^{-1} as per Biswas and Mishra (2015) (9):

$$q_B = Qv \left(Co - \frac{CB}{2} \right) \frac{tB}{M} \tag{9}$$

where Qv (L min^{-1}) denotes the flow rate of influent, Co (mg L^{-1}) represents ionic concentration of influent, M (g) denotes mass of the filter bed, CB (mg L^{-1}) symbolises heavy metal concentrations at breakthrough point, whereas t$_B$ (minutes) denotes breakthrough time.

2.9. Analysis of column kinetics

The behaviour of clay brick waste as an adsorbent on column adsorption of heavy metal ions from aqueous solution was described through column kinetic modelling. In this study, Yoon-Nelson and Thomas kinetic models were applied.

2.9.1. Yoon - Nelson model

According to Bharathi and Ramesh (2013); Singh et al. (2015), Yoon-Nelson kinetic model is commonly applied in a wide range of ionic concentrations of the solution between saturation and breakthrough time with supposition that the probability of rate of adsorption to decrease in every molecule of a contaminant is proportional to that of breakthrough and sorption of adsorbate. The linearized form of the Yoon-Nelson model Eq. (10) described by Lekgoba et al. (2020).

$$t = \tau \frac{1}{kYN} \ln \frac{Ce}{Co - Ce} \tag{10}$$

1- Submersible pump, 2- Influent tank, 3- Valve, 4- Water rotameter

5- Water level, 6- Bed (Adsorbent), 7- Sampling point, 8- Storage tank
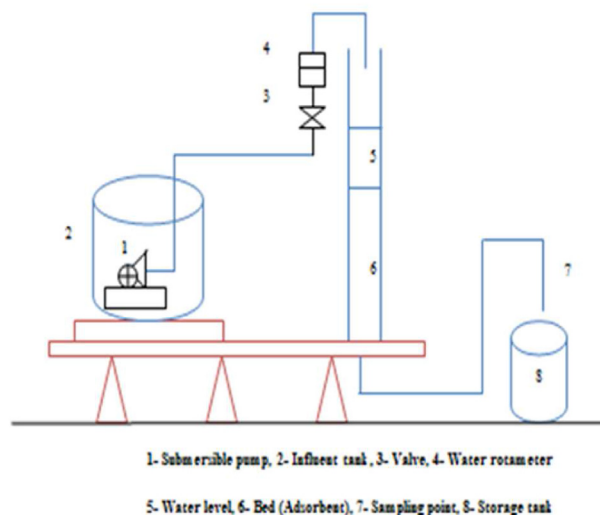
Figure 1. Experimental setup of column adsorption.

where t is the sampling time (minutes), τ (minutes) denotes time required to reach 50% breakthrough, and KYN denotes rate constant (per minute).

2.9.2. Thomas model

According to Singh et al. (2015), the Thomas model is a column adsorption kinetic model which is mainly used to compute column adsorption performance and estimate breakthrough curves. The model assumes that the process follows Langmuir kinetics (Rajeshkannan et al., 2013). The limitation of the model is that it follows second order kinetics, so there is no restriction of chemisorption (Bharathi and Ramesh, 2013). The following is a linearized mathematical equation of Thomas kinetic model (11) described by Biswas and Mishra (2015).

$$\ln\left(\frac{Co}{Ce} - 1\right) = \frac{KTH\ qoM}{Q} - \frac{KTHCoV}{Q} \tag{11}$$

where KTH (mL min^{-1} mg^{-1}) represents the Thomas rate constant, q$_o$ denotes the heavy metal uptake per g of the media (mg g^{-1}). M (g) denotes the mass of clay brick waste, Co represents ionic concentration of the influent (mgL^{-1}), Ce denotes the effluent concentration at time t (mgL^{-1}), and V denotes the flow rate (mLmin^{-1}).

2.10. Regeneration or reusability studies

The objective of the regeneration study is to restore the retention capacity of the media and the recovery of some important ions (Hu et al., 2005). The commonly used and effective 0.1M sodium hydroxide (NaOH) was used as the regeneration eluent in this study. Desorption experiments were conducted in three consecutive regeneration cycles and the desorption was computed using the following Eq. (12) as described by Letina and Letshwenyo (2018).

$$\text{Desorption}(\%) = \frac{Ci - Ce}{Ci} X100 \tag{12}$$

3. Results and discussions

3.1. Characterisation of adsorbent

3.1.1. X-Ray Diffraction of the adsorbent

Figure 2 illustrates the mineralogical phases present in the clay brick adsorbent before and after adsorption of heavy metals. Kapur and Mondal (2014) reported that the crystalline and amorphous phases are each represented by wide and sharp peaks in the diffraction pattern. In this study, crystalline mineral phases of the two minerals; Quartz and Mullite were clearly shown by sharp peaks in the XRD pattern. The crystalline minerals accounted for 51.28% and 23.4% of Quartz and Mullite, respectively, and the remaining composition was of amorphous minerals. In addition, Chancey et al. (2010) found that the sharp peaks of crystalline minerals, illustrated at an angle of approximately 26.6° in the XRD pattern indicate that the material is predominantly amorphous. In this case, it can be observed that there is a sharp peak closer to an angle of 26.6°. Therefore, it can be concluded that the adsorbent was amorphous.
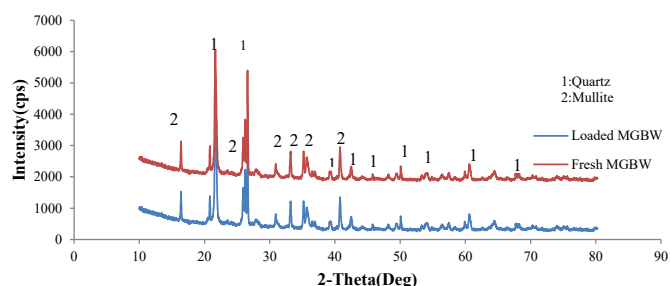

Figure 2. X- Ray Diffraction pattern of fresh and loaded adsorbent.

Further observations can be made that there were no significant changes in the pattern before and after adsorption of heavy metal ions. The diffraction patterns of this study are comparable to the XRD patterns of the studies conducted by Macías-Quiroga et al. (2018), Ouyang et al. (2019).

3.1.2. Elemental analysis, leaching and surface morphology

Different elemental concentrations of the clay brick waste as an adsorbent are illustrated in Table 4.

According to Arias et al. (2003), various elements such as iron and aluminium can compete with other coexisting ions present in water for active sites. The results of the elemental analysis revealed that the fresh adsorbent had an iron content of 1.78 mgL^{-1} and 2.66 mgL^{-1} and the elemental concentrations dropped to 2.53 mgL^{-1} and 1.34 mgL^{-1} for iron and aluminium, respectively. The drop can be attributed to leaching or ion exchange that occurred during the adsorption process. Leaching results showed that all leachate concentrations were below the regulatory limits set by the Botswana Standards (BOS) for aquatic systems (Table 5). Therefore, it can be concluded that the clay brick waste is a non-hazardous material. The surface morphology of the media was also performed before and after heavy metal loading. It can be observed that clay brick waste used as an adsorbent had micro pores and uneven surfaces before and after adsorption (Figure 3). The more porous media is not always characterised by high pollutant affinity, but the surface chemistry (Drizo et al., 1999).

#### 3.1.3. Thermogravimetric analysis (TGA)

The purpose of the thermogravimetric analysis was to investigate the thermal stability and the 0.51% weight loss during heating at temperatures closer to 100 °C can be attributed to the evaporative removal of physically adsorbed humidity on media (Favero et al., 2016,; mineralogical changes that the adsorbent can undergo during heating (Macías-Quiroga et al., 2018). The fresh and loaded adsorbent was heated from room temperature to approximately 1000 °C at a heating rate of 15 °C per minute as per Zyoud et al. (2020). The thermographs in Figure 4 illustrate the weight loss of the fresh, heavy metal loaded clay brick waste during heating. It can be observed that the fresh and loaded clay brick waste brick had total mass losses of 2.15% and 2.255%, respectively. Approximately Zyoud et al., 2020). In addition, it can be observed that at temperatures between 100 °C and 200 °C, the fresh adsorbent revealed mass loss of approximately 0.20% which may be associated with coordinated moisture loss (Janbuala and Wasana-piarnpong, 2015). Further observations can be made that the mass loss at temperatures exceeding 200 °C was 1.35% and chemical bonds were broken at such temperatures. A comparison can be made with

**Table 4.** Elemental concentrations of fresh and loaded adsorbent.

Elements (mgL^{-1})	Fresh MGBW	Loaded MGBW
Al	2.66 ± 0.14	2.53 ± 0.06
Si	8.74 ± 1.45	7.53 ± 0.07
K	0.72 ± 0.08	0.44 ± 0.17
Ca	2.28 ± 0.09	1.48 ± 0.45
Ti	0.23 ± 0.01	0.19 ± 0.03
Cr	0.03 ± 0.01	-
Mn	0.03 ± 0.02	0.05 ± 0.02
Fe	1.78 ± 0.25	1.34 ± 0.09
Co	-	-
Ni	-	-
Cu	-	0.02 ± 0.00
Zn	0.01 ± 0.00	0.01 ± 0.0019
Pb	0.004 ± 0.00	0.003 ± 0.001
As	0.001 ± 0.00	-

Table 5. Leachate concentrations from fresh adsorbent.

| Adsorbent	Heavy metal concentration (mgL^{-1})	Leaching time (hours)		
MGBW	Cu	0.18 ± 0.03	0.05 ± 0.01	0.016 ± 0.001
	Fe	0.02 ± 0.001	0.005 ± 0.001	0.074 ± 0.002
	Ni	0.003 ± 0.001	0.002 ± 0.0001	0.25 ± 0.01
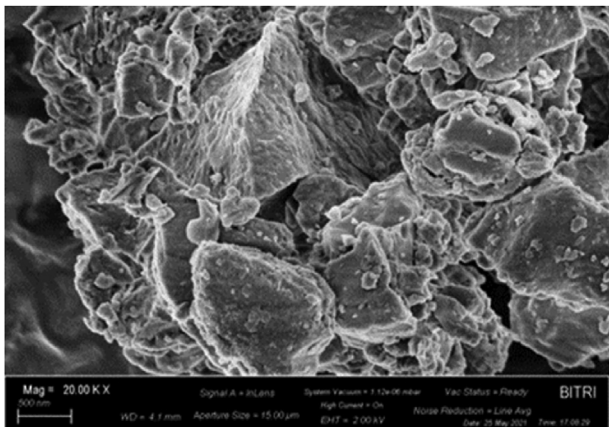
a) Before adsorption
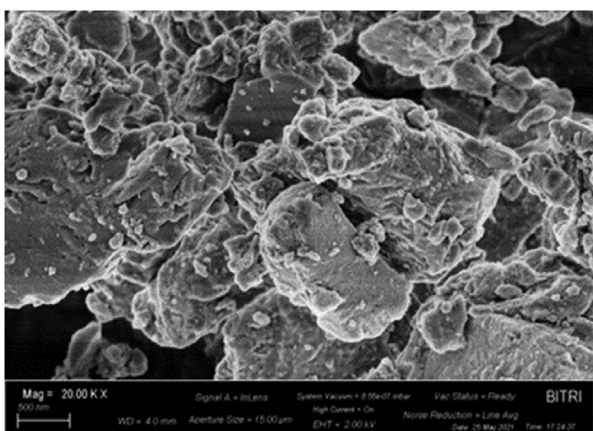
b) After adsorption

Figure 3. SEM images of clay brick waste before (a) and after (b) heavy metal adsorption.

thermographs reported by Zyoud et al. (2020) (Favero et al., 2016), (Macías-Quiroga et al., 2018) (Janbuala and Wasanapiarnpong, 2015).

3.1.4. Fourier transform infrared (FTIR) measurements

Figure 5 represents the infrared spectral bands for the functional groups of found in the fresh and loaded MGBW. It can be observed that there is no significant difference in the spectral bands before and after adsorption of heavy metals. The spectral band positioned at approximately 468 cm^{-1} indicates the presence of Si–O bending, Si–O–Fe stretching functional group, and it shows silicon-oxygen bonding and Silica-Iron bonding. The Si–O stretching, (Al, Mg)–OH, Si–O-(Mg, Al) are represented by the spectral peak at approximately 796cm^{-1}. The peak at
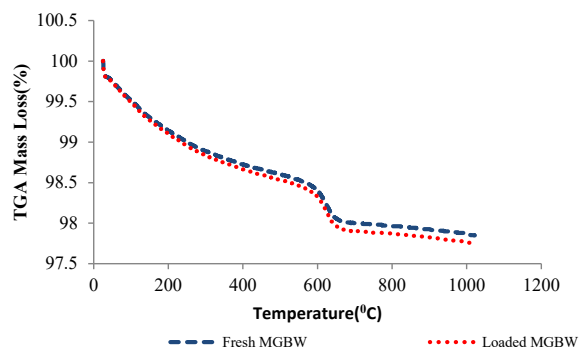
Figure 4. Thermograph of fresh and heavy metal loaded adsorbent.

881 cm^{-1} is likely to represent a weak Al–Mg–OH deformation. The infrared spectral band at 1081 cm^{-1} represents stretch vibration modes of SO$_4$ tetrahedral. Lekgoba et al. (2020) have reported the band range 500–1500 cm^{-1} as a finger print region where there is complexity in visual reading and interpreting specific compounds formed during adsorption. However the comparison of spectral bands allows for easier establishment of identity of specific compounds formed during adsorption. A comparison can be made between the spectral band of MGBW and other materials used by (Jozanikohan and Nosrati, 2022), (Rüscher et al., 2022) where clay and Alkali-Activated Slags and CEMI/CEMIII Pastes were respectively used.

3.1.5. The effect of contact time

The adsorption capacities of the media with respect to time for the uptake of Cu^{2+}, Fe^{2+}, and Ni^{2+} from the solution to the adsorbent are shown in Figure 6. The rate of the adsorption process initially depends on the mass transfer stage (Wierzba, 2017). The initial phase is characterized by high intense adsorption due to the availability of active sites on the surface of the adsorbent, hence the large concentration gradient activates the process (Wierzba, 2017). It can be observed that the initial stage of mass transfer from the solution to the surface of the media lasted approximately 30 min for the adsorption of Cu^{2+}, Fe^{2+}, and Ni^{2+}. The equilibrium started thereafter and was more pronounced at 60 min, which was adopted as the optimum time with adsorption capacities of 7.6, 6.7 and 6.2 mg g^{-1} media (Figure 6). However, different authors reported optimum contact times for the sorption of Cu^{2+}, Fe^{2+}, and Ni^{2+} (Osińska, 2017; Ouyang et al., 2019). The main reason for the differences in the optimum contact times and adsorption capacities could be the differences in the media mineralogy and concentration of metals.

3.2. Batch kinetic models

It can be noted that the removal of Cu^{2+}, Fe^{2+} and Ni^{2+} using MGBW follows PSO with RMSE values of 0.11, 0.06 and 0.14, respectively (Table 6). According to Martins et al. (2014), when the adsorption process obeys the PFO kinetic model, the adsorption takes place through diffusion between the interface. The Lagergren PSO kinetic model implies that the chemisorption is the rate controlling mechanism, such that there was chemical bonding that occurred between the media surface and the metals (Mishra et al., 2017). The adsorptive removal of Cu^{2+}, Ni^{2+}, and Fe^{2+} on the adsorbent indicated that the chemisorption process was taking place.

3.3. Intraparticle diffusion model

The plot of the intraparticle diffusion model was used to further investigate the adsorption mechanisms involved in the heavy metal removal (Figure 7). If the plot of qt vs t^{½} is a straight line passing through the origin, then the adsorption process is controlled solely by the intraparticle diffusion (Fierro and Torne, 2008). It can be observed that the
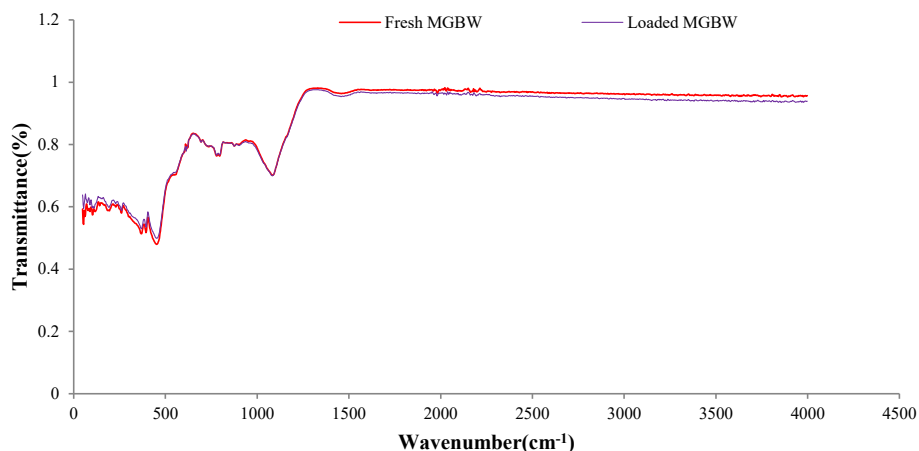
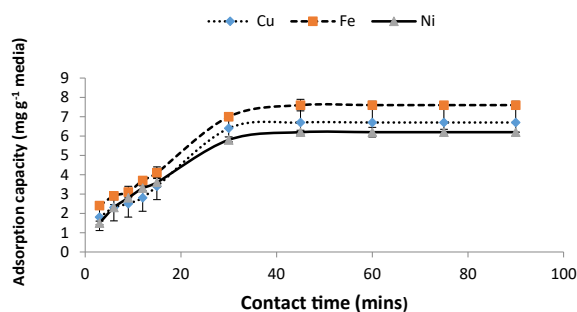**Figure 5.** FTIR spectral bands for fresh and used MGBW.

Figure 6. The effect of contact time on adsorption of Cu $^{2+}$, Fe $^{2+}$ and Ni $^{2+}$.

evidence that there were two or more steps controlling the sorption processes. The intercept gives an indication of the thickness of the boundary layer (Fierro and Torne, 2008) that should be overcome during mass transfer. It has been reported by (Viegas et al., 2014) that the rate-limiting step during adsorption processes helps determine of practical options that should be introduced to improve the system. Since film diffusion is the rate-limiting step, turbulent conditions or mixing can be improved by increasing mixing or stirring speed. In the case of intra-particles, the rate-limiting step adsorbent dose can be increased for more adsorption sites. Therefore, in this study, it was evident that both the stirring speed and the media dose could be increased to improve the adsorption process.
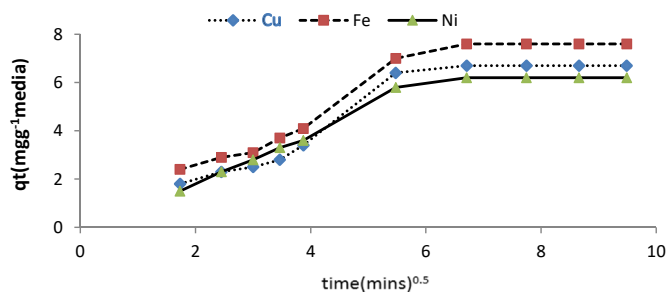
adsorption of the three ions onto MGBW indicates three distinctive steps involved during the process (Figure 7). The rate constants for the first and second steps during Fe^{2+} adsorption were 0.73 and 1.2 mg g^{-1} min$^{-0.5}$. In the case of Cu^{2+} adsorption, the corresponding rate constants were 0.8 and 1.82 mg g^{-1} min$^{-0.5}$. In both scenarios, the rate constants of the first stages (film diffusion) were lower than the rate constants of the second stages (intra-particle diffusion), indicating that film diffusion controlled the rate of Fe^{2+} and Cu^{2+} ions adsorption in MGBW. These findings are similar to those observed by Jellali et al. (2011) for phosphate ions adsorption in phosphates mine wastes. The rate constants for Ni^{2+} adsorption were 1.02 and 0.9 mg g^{-1} min$^{-0.5}$ for instantaneous and gradual adsorption. In contrast to the other two ions (Cu^{2+} and Fe^{2+}), the gradual adsorption controlled the rate of the adsorption mechanism. All the graphs have the intercept C indicating that they did not pass through the origin, so intraparticle diffusion did not solely control the rate of adsorption. The multi-linearity exhibited by all the graphs is further

Figure 7. The Intra-particle diffusion kinetic model.

Table 6. Adsorption constant rates and correlation coefficients for Pseudo-First Order, Second Order rate equations and the Intraparticle diffusion model parameters.

Adsorbent	Pseudo-First Order Kinetic Model						Pseudo-Second Order Kinetic Model				
	Metal Ions	q $_e$ model (mgg^{-1})	q $_e$ experimental (mg g^{-1})	k$_1$ (min^{-1})	R^2	RMSE	q $_e$ model (mgg^{-1})	q $_e$ experimental (mgg^{-1})	k$_2$ ((g/mg) min)	R^2	RMSE
MGBW	Cu^{2+}	3.61	6.7	0.06	0.98	0.9999	10	6.7	5	0.97	0.11
	Fe^{2+}	4.46	7.6	0.07	0.96	0.9999	10	7.6	6.67	0.98	0.06
	Ni^{2+}	4.01	6.2	0.12	0.997	0.9999	10	6.2	5.88	0.99	0.14

Intraparticle Diffusion kinetic Model				
Adsorbent	Metal Ions	K$_{id}$ (mg/(gmin$^{-0.5}$))	C	R^2
MGBW	Cu^{2+}	0.74	0.70	0.87
	Fe^{2+}	0.78	1.25	0.89
	Ni^{2+}	0.64	1.03	0.88

3.4. Equilibrium studies

3.4.1. The effect of adsorbent dosage

The adsorbent dose influences the capacity of adsorption and the removal efficacy of media. The effect of adsorbent dosage ranging from 0.5 g to 6.0 g was investigated for the removal of Cu^{2+}, Fe^{2+}, and Ni^{2+} onto MGBW (Figure 8). The maximum adsorption capacity of Cu^{2+}, Fe^{2+}, and Ni^{2+} was achieved at a dose of 2.0 g. The order of magnitude was observed as Fe^{2+} removal was 1.12 more than Ni^{2+} removal which was 1.08 times more than Cu^{2+} removal. The initial increase in percent removal as the adsorbent dose was increased from 0.5, 1.0 and 2.0 g because of increased accessibility of many active sites or increase in surface area of the adsorbent is comparable to the observation made by Gebretsadik et al. (2020). The results are also comparable to the findings reported by Ouyang et al. (2019). The drop in capacity of adsorption as observed later was because of decrease in the concentration of adsorbates (Jia et al., 2003). It has been reported that an increase in adsorbent dose, and aggregation of adsorbent particles hinders the adsorption process due to overlapping of adsorption sites. This aggregation reduces the surface area of the adsorbent resulting in reduction of the adsorption process of the metal ions (Nithya et al., 2018).

In contrast, the maximum adsorption capacities of 10, 7.6 and 7.2 mgg^{-1} media were observed at a dose of 0.5 g (5.0 gL^{-1}), Figure 9 and it can be observed that there is an inverse relationship between the adsorbent dose and the adsorption capacity. It has been reported that at a high adsorbent dose there is a possibility of aggregation of adsorbent which reduces the surface area and thus reduces metal ions uptake (Nithya et al., 2018). It was observed that the adsorption capacities of the metal ions decreased with increasing adsorbent dose.

3.4.2. Adsorption isotherms

The adsorptive removal of Cu^{2+} on MGBW at temperatures of 293K and 303K followed the Langmuir isotherm better than the Freundlich isotherm. The K_L at 293K was higher than at 303K, indicating that Cu^{2+} had a stronger affinity for the adsorbent surface at 293K than at 303K. The adsorption of Cu^{2+} at 313K obeyed Freundlich isotherm with R^2 values of 0.9056 and 0.8830 for the Langmuir models. The Freundlich model described Fe^{2+} and Ni^{2+} adsorption better than the Langmuir model at both temperatures (Table 7). The results suggest that the surfaces were heterogeneous and that the active sites on the adsorbent had different energies (Balouch et al., 2015). It has been reported that values of $1/n < 1$ indicate a favourable adsorption process, and also n values ranging from 1 to 10 indicate a good adsorption process and a favourable physical process (Al-Senani and Al-fawzan, 2018). The values of $1/n$ were all <1, thus indicating favourable adsorption of the metal ions. It can also be concluded that the MGBW surfaces were also heterogeneous with exponentially distributed energy levels on the active sites. The adsorption intensity values, n, ranged from 1.15 and 2.16 indicating a good adsorption process. These results contrast with the findings of Abdel et al. (2011) whose data fit the Langmuir model better than the Freundlich model for the removal of heavy metals from

Figure 8. The effect of adsorbent dosage on heavy metal removal.

wastewater using low-cost adsorbents. However, the study is comparable to the study conducted by Wang et al. (2020) on the adsorptive removal of divalent copper and cadmium ions from the aqueous solution using Na^+ modified Pisha Sandstone. Furthermore, the results are comparable to the findings reported by Hemalatha and Rao (2014) where the data fit both the Langmuir and Freundlich model satisfactorily for the sorption of hexavalent chromium and nickel in calcined brick powder. The study is also comparable to the work reported by (Ouyang et al., 2019) on the removal of Pb^{2+}, Cd^{2+}, and Cu^{2+} using silicate tailings.

3.4.3. The effect of initial pH

The influence of pH on heavy metals adsorptive removal by MGBW is illustrated in Figure 10. The solution pH is a crucial parameter for the adsorption of metal ions as it has an impact on the adsorbate solubility and the degree of ionisation of the adsorbates during adsorption (Sharma and Bhattacharyya, 2005). The pH also affects the surface charge of the adsorbent, which in turn influences which ions of adsorbate (anions or cations) are adsorbed or exchanged. The impact of pH was examined in the pH range from 2 to 12. It was observed that the optimum pH was 8.0 for the adsorption of Fe^{2+} on MGBW with 76% removal, pH 10 and pH 6 for Cu^{2+} and Ni^{2+} removal, respectively with 70% and 64% removal efficiencies (Figure 10). The optimum pH was similar to the pHpzc, which was 8.33, and an increase in pH after optimum value shows a decrease in percentage removal of the three metal ions. The results are comparable to the findings of Bagali et al. (2017) who observed a decrease in lead $^{2+}$ removal from the aqueous solution using Banana Pseudostem. There might have been high proton concentrations which then minimised adsorption of heavy metal ions as reported by Lai et al. (2010), but metal precipitation was favoured at pH values higher than pHpzc. The same was reported by Farhan and Khadom (2015) concluded that at low pH, protons compete with metal ions for the available active adsorption sites responsible for the uptake of metal ions, resulting in a decrease in the metal ions adsorption.

Low adsorption capacities were observed at low pH and this is associated with high concentrations of H^+ ions in the solution, which compete with positively charged metal ion. The adsorption capacities have been observed increase with increasing pH as the competition of H^+ ions (Kong et al., 2019). The main adsorption mechanism that might have promoted the metal uptake in the low pH range, or it might have been due to the ion exchange and electronic attraction and metal precipitation at elevated pH values (Benzaoui et al., 2018). The results are also similar to the observation by Nie (2021) on the adsorption of metal ions from wastewater into a multifunctional metal-organic- frame work based trap. The competition decreased as pH increased, which caused the negatively charged adsorbent surface active sites to promote the removal of the positively charged metal ions (Ouyang et al., 2019). The highest removal efficiencies were 76%, 67% and 64% for Fe, Cu and Ni ions, and the corresponding pH values were 8, 8 and 6, respectively. In the case of Fe and Cu ions, the pH values were closer to the point of zero charge, which reduced the competition between the metal ions and protons and thus promoted the adsorption of these metal ions in the adsorbent (Foroutan et al., 2020). The observed decrease in adsorption efficiency with increasing pH could be due to the formation of insoluble metal hydroxides at high pH values as reported by Nithya et al. (2018) on the adsorption of Ni^{2+} on green extract capped superparamagnetic iron oxide nanoparticles. The same was reported by Bakhtiari and Azizian (2015) that at pH values greater than 6, copper ion precipitates as copper hydroxide Cu $(OH)_2$. The removal of Fe ions from the solution at high pH values could be due to their hydrolysis and precipitation reactions of the hydrolysed products such as ferric hydroxides (Nosrati et al., 2009), and this could have been the case in this study. Although not investigated in this study, the report by Nosrati et al. (2009) suggested that the ionic concentration of Fe decreases with increasing pH, which could be due to hydrolysis and precipitation, hence the decrease in Fe removal observed in this study.
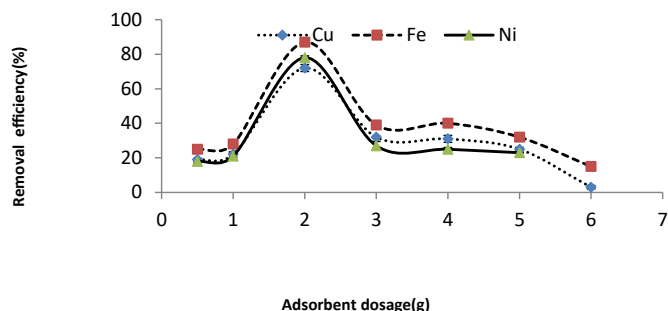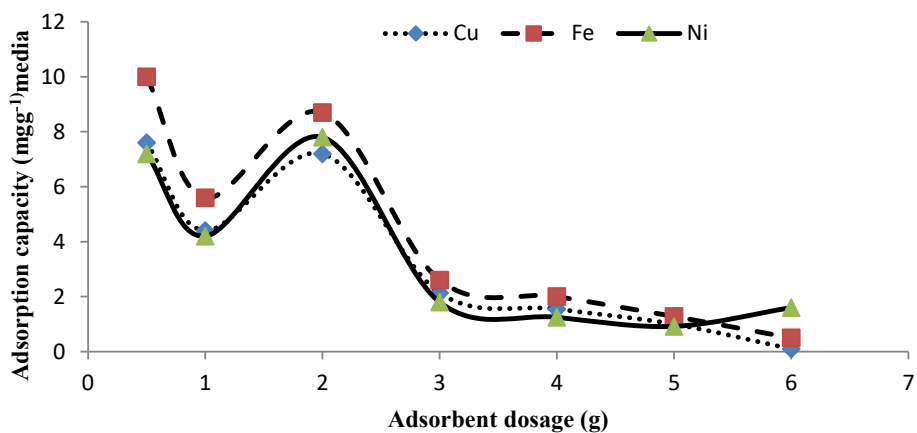
Figure 9. Adsorbent dose vs adsorption capacities of Cu, Fe and Ni ions onto clay brick waste.

Table 7. Constants of Langmuir and Freundlich isotherm models.

| Adsorbent	Heavy metal ions	Temp(K)	Langmuir constants				Freundlich constants		
			q_{max} (mgg^{-1})	K_L (Lmg^{-1})	R^2	R_L	K_f (mgg^{-1})	1/n	R^2
MGBW	Cu^{2+}	293	2.29	0.81	0.95	0.07	0.81	0.56	0.87
		303	2.60	0.55	0.97	0.01	0.74	0.59	0.89
		313	1.94	0.35	0.88	0.01	0.42	0.70	0.90
	Fe^{2+}	293	1.72	0.23	0.52	0.022	0.29	0.77	0.79
		303	0.73	3.46	0.12	0.001	0.43	0.59	0.64
		313	0.75	1.53	0.07	0.003	0.32	0.63	0.65
	Ni^{2+}	293	0.57	12.90	0.004	0.0004	0.61	0.47	0.34
		303	0.52	24.51	0.001	0.0002	0.55	0.46	0.31
		313	1.27	0.10	0.36	0.05	0.16	0.87	0.58
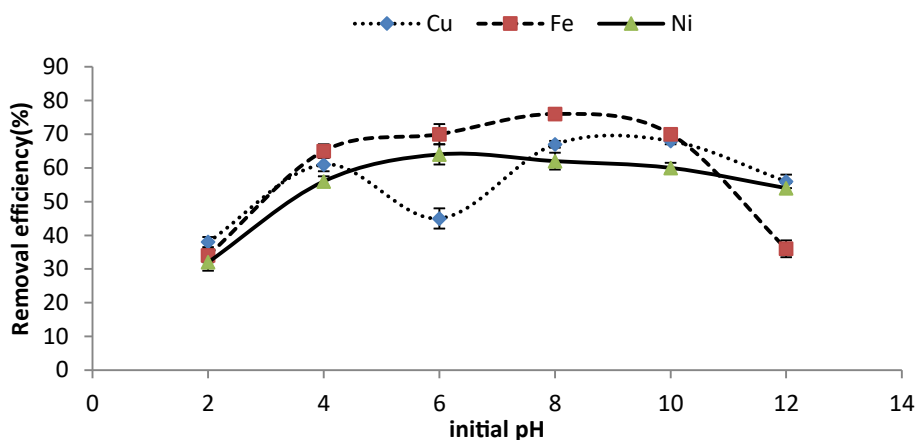
Figure 10. The effect of initial pH on Cu^{2+}, Fe^{2+} and Ni^{2+} removal.

There are differences in the adsorption capacities of the three metal ions due to their competition effect. Properties of metal ions, such as the ease of the hydrolysis, contribute to their removal efficiency (Adebowale and Unuabonah, 2005). Figure 10 indicates that at different pH values, Fe ions hydrolysed more than the other two metal ions, with Cu ions coming second, except at pH 6 when Cu^{2+} was the second better adsorbed metal ions. Some of the properties of metal ions that influence their adsorption are the ionic potential, electronegativity, and softness capacities of these metal ions (Ouyang et al., 2019). A study conducted by Charazi'nska et al., (2021) reported the order of removal efficiency of some heavy metals in Polish peats in the order Fe(III) > Cr(III) > Cu(II) > Ni(II) similar to this study, when the effect of pH was investigated (Figure 10).

Some studies have been conducted, for example, it was reported that Pb ions had more affinity for modified rice husk than Cu ions in multi component solutions, and the stability and enthalpy of formation are greater for Pb^{2+} ions than for Cu2+ ions modified rice husk (Ahmar-uzzaman, 2011).

Figure 11 shows the pH pzc of clay brick at pH 8.3. According to Mushtaq et al. (2014), the point of zero charge is defined as the point where the surface charge density is zero. It has been reported that the surfaces of media are negatively charged at solution pH values greater than pH pzc (Tran et al., 2017a, b). The adsorbent surface acquires positive charges when the pH of the solution is < pH pzc. The adsorption of heavy metals in this case can be favoured at a pH higher than 8.3 due
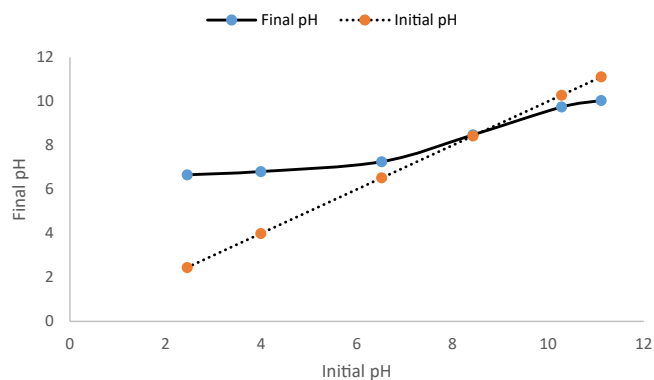
Figure 11. The pH pzc of the fresh clay brick adsorbent.

to the electrostatic force of attraction between the adsorbent surface and the adsorbates. It is not always a guarantee that adsorption of metal ions will be favoured at a solution pH higher than pHpzc due to mineralogical changes caused by some environmental factors such as precipitation, acid rain, and solar radiation. The results are comparable to the findings by Mushtaq et al. (2014), Hajira et al. (2018).

3.5. Thermodynamic studies

The adsorption thermodynamic variables for the adsorptive removal of Cu^{2+}, Fe^{2+} and Ni^{2+} in MGBW are summarised in Table 8. The table also summarises Gibbs free energy (ΔG^o), enthalpy (ΔH^o) and entropy (ΔS^o) values at 293K, 303K, and 313K. All ΔG^o values were positive, indicating that the adsorption of all metal ions was a non-spontaneous process. The negative values of ΔS^o indicate that the movement of all metal ions to the surface of the media did not require energy, so the process was endothermic (Alanber, 2011). This is contrary to the findings reported by Lekgoba et al. (2020) where fly ash was used for the adsorption of Ni^{2+} and Cu^{2+} from aqueous solutions. There was a low degree of freedom at the interface since the adsorption reactions are expedited at all temperatures, compared to the findings by Bouhamed et al. (2012). The heats of adsorption for van Edward force, hydrogen bond, ligand exchange, dipole interaction, and chemical bond range are reported as 4–10, 2–40, $\approx$40, 2–29, and >60 kJ·mol^{-1}, respectively. The adsorption onto MGBW ranged from 5 to 10, indicating van Edward force. Negative values of ΔS indicated low affinity of the adsorbent for the heavy metal ions, while positive values of ΔH indicate endothermic reactions (Xu et al., 2017). The findings suggest that at high temperatures, the adsorption surfaces are activated and enlarged, promoting the formation of more active sites for the adsorption of the metal ions (Rahman and Sathasivam, 2015). In addition, the high temperatures promote high mobility of metal ions from the bulk solution to the adsorbent surfaces, thereby facilitating the adsorption process.

3.6. Fixed bed column adsorption studies

The prediction of adsorption breakthrough curves is necessary in the design of column adsorption treatment systems (Malkoc and Nuhoglu, 2006). In this study, clay brick waste was used as an adsorbent for Fe^{2+}, Cu^{2+} and Ni^{2+} from a multiple element solution from the initial concentration of 200 mgL^{-1}. The influent was pumped at a discharge rate of 0.02 Lmin^{-1} and the adsorbent was packed at a height of 29cm breeding a bed volume equivalent to 0.01 m^3. The breakthrough curve (concentration – time profile) for column adsorption is shown in Figure 12. It can be noted that the ionic concentration of nickel was higher than the concentrations of divalent copper and iron for 5670 min. The low adsorptive removal of divalent Nickel ions from the multicomponent solution may be attributed to its low electronegativity and large ionic radius compared to the divalent copper and iron ions (Table 9). According to Osińska (2017), a large ionic radius and low electronegativity of the contaminant reduce diffusion rate of the contaminant into active sites of the adsorbent.

The concentration-time profile in this study also showed a higher concentration of Ni^{2+} in the treated effluent, exceeding the initial concentration of 200 mgL^{-1}. This may be associated with the leaching of Nickel from the media as well as the unavailability of exchangeable sites for Nickel. However, it is worth noting that Cu^{2+} was adsorbed in large quantities until 5040 min, and after 90 minutes from 5040 min, high concentrations of copper ion of 2.43 and 12.36 mgL^{-1} were noted after 5130 and 5220 min, respectively. The concentrations of Cu^{2+} then decreased, resulting in high Cu^{2+} removal. Such a high adsorptive Cu^{2+} removal may be attributed to small ionic radius and higher electronegativity, resulting in high diffusion rate and saturation rate of adsorbate on the surface of media (Osińska, 2017; Lekgoba et al., 2020). However, it can be noted that Fe^{2+} was also highly adsorbed due to the large number of exchangeable active sites on the adsorbent surface (Gebretsadik et al., 2020). Some studies have reported that the breakthrough point is chosen randomly at some arbitrary contaminant concentrations (Lekgoba et al., 2020). In this study, 1.0 mgL^{-1} was chosen as a consent value for copper and nickel, while 2.0 mgL^{-1} was selected for iron, based on the Botswana Standards (BOS) for the discharge of industrial effluent in perennial and ephemeral streams. The adsorption capacities of MGBW at the end of the experiment were found as 2.22 mgg^{-1} media, 2.23 mgg^{-1} media and 0.74 mgg^{-1} media for Cu^{2+}, Fe^{2+} and Ni^{2+}, respectively.

The adsorbent is considered saturated or exhausted at concentrations of approximately 90% of the initial concentration (Lekgoba et al., 2020). In this study, only nickel reached saturation, and at times desorbed copper and iron required more time to reach saturation (Figure 12). It is anticipated that the adsorption capacities for these ions will have been higher if the experiments had been conducted to breakthrough for C^{2+} and Fe^{2+}. The amount of treated effluent was equivalent to 113400 mL (113.4 L). In conclusion, clay brick waste can be used as an effective adsorbent for the removal of divalent copper and iron, but not nickel, from industrial effluents before discharge into aquatic environments.

Table 8. Thermodynamic parameters for the adsorption of Cu^{2+}, Fe^{2+} and Ni^{2+}.

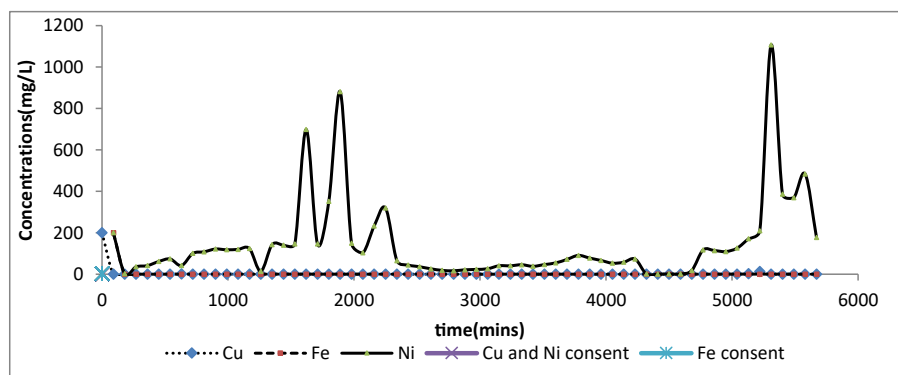| Adsorbent	Metal ion	Temperature (k)	ΔG^o (kJmol^{-1})	ΔH^o(kJmol^{-1})	ΔS^o(kJmol^{-1}K^{-1})
MGBW	Cu^{2+}	293	5.572		
		303	5.819	5.205	-0.037
		313	6.313		
	Fe^{2+}	293	6.105		
		303	6.816	9.322	-0.054
		313	7.168		
	Ni^{2+}	293	4.490		
		303	4.772	5.222	-0.033
		313	5.154		

Figure 12. Breakthrough curves (concentration-time profile) for sorption of Ni $^{2+}$, Fe $^{2+}$ and Cu $^{2+}$.

Table 9. Chemical properties of metal ions (Bohli, 2013).

Heavy metal ion	Atomic weight (A_r)	Ionic Radius (A^o)	Electronegativity	Hydrated-Radius (A^o)
Ni^{2+}	58.7	0.72	1.91	4.04
Cu^{2+}	63.5	0.69	2.00	4.19

3.6.1. Column adsorption kinetic models

In this study, the description of the adsorption behaviour of heavy metals on clay brick waste adsorbent in a fixed - bed column was performed using the Thomas or reaction model and the Yoon-Nelson model. According to Trgo et al. (2011), the Thomas or reaction model is derived based on a second order kinetics, assuming that the adsorption process follows Langmuir kinetics. On the other hand, Yoon-Nelson kinetic model works in a range of ionic concentrations to express the breakthrough time and the saturation time of the adsorption process (Sarma et al., 2019). The column results showed similar determination coefficients (R^2) values of 0.06 and 0.07 for the adsorption of divalent copper, and iron, respectively (Table 10).

This indicates that the adsorption of heavy metals follows the two models. The Ţ value in Yoon-Nelson model is a measure of the time it takes to reach 50% of contaminant breakthrough (Biswas and Mishra, 2015). In this case, the Yoon- Nelson model indicated that 23846.33 minutes (397.44 h), 18145 minutes (302.42 h) and -13952 minutes (−232.53 h) were required to reach 50% Cu^{2+}, Fe^{2+} and Ni^{2+} breakthrough, respectively (Table 10). The negative values of Ţ for nickel sorption can be attributed to excessive leaching of Nickel on the media. This fixed column adsorption study is comparable to fixed-bed column studies by (Biswas and Mishra, 2015) (Haile and Fuerhacker, 2018) (Lekgoba et al., 2020). Table 11 shows the performance of other adsorbents in column adsorption studies.

3.7. Reusability studies

According to Zhang and Wang (2015), reusing or regenerating the used adsorbent is economically imperative because it minimises media replacement costs. Hu et al. (2005) reported that the main objective of regeneration studies is to restore the adsorption capacity of the used adsorbent and for the recovery of some important adsorbed components. It can be observed that fresh clay brick waste had an initial removal efficiency of 67 ± 0.63,76 ± 0.72 and 62 ± 0.63% for Cu^{2+}, Fe^{2+} and Ni^{2+}, respectively (Figure 13). The Cu^{2+} removal efficiency of the clay brick waste adsorbent was reduced to 63%, 61 % and 57% in the first, second and third reusability cycles. In addition, the Fe^{2+}removal efficiency of the clay brick also decreased to 66%, 54% and 43% in the first, second and third regeneration trials. A drop in Ni^{2+}removal efficiency was also observed as 51%, 42% and 39% in the first, second and third reusability trials. Zhang and Wang (2015) also observed a drop in Ni^{2+} removal

efficiency when using Nano-composite of lignocellulose/montmorillonite as an adsorbent. Such a decrease in removal has been attributed to an increase in temperature (Gill et al., 2013; Zhang and Wang, 2015). In the regeneration study by (Ahmad et al., 2012), it was found that desorption of divalent copper increased in other cycles where 0.1M hydrochloric acid (HCL), 0.1M Ethylenediaminetetraacetic acid (EDTA) and 0.01M sodium Hydroxide (NaOH) was applied as effluents on iron-oxide coated eggshells. An increase in desorption may be attributed to ion exchange and loss of adsorption active sites generated by the acids used (Ahmad et al., 2012). In conclusion, the clay brick waste adsorbent (MGBW) showed a promising reusability potential, which can reduce the cost of adsorbent replacement.

3.8. Adsorption mechanisms of metal removal

Figure 14 shows a simplified schematic diagram of adsorption mechanisms by MGBW. Adsorption mechanisms for contaminant removal are related to important parameters such as adsorption isotherms and kinetics. Such parameters are useful during the design and construction of water and wastewater treating systems. Exchangeable metal ions such as calcium (Ca) and potassium (K) in the adsorbent were released from the adsorbent to the solution and were replaced with other metals. This indicates that the cation exchange process occurred during adsorption by MGBW. The chemical reactions that took place during adsorption may have formed some precipitates at high pH levels, hindering the binding of metals to active sites. According to (Mishra et al., 2017), the adsorption process is considered to be chemisorption if it follows the pseudo second order kinetic model. In this case, the adsorption process followed the pseudo second order kinetic model, suggesting that chemisorption was the dominant process. Furthermore, the interaction of heavy metals with some functional groups present in MGBW such as Si–O–Fe, Si–O might have favoured the binding of metals to the active sites of the media. The stretch vibration modes of SO$_4$ tetrahedral detected by FTIR in MGBW before and after adsorption of heavy metals indicate that SO4 from the salts used to prepare the adsorbate did not cause any chemical reaction during sorption as nothing different from the spectral peaks was noted. The interaction mechanisms of metal removal can be compared to those reported by (Lekgoba et al., 2020) who used coal fly ash as an adsorbent for copper and nickel removal (Letshwenyo and Mokokwe, 2021), who used acid washed copper smelter slag for sulphates and phosphorus removal.

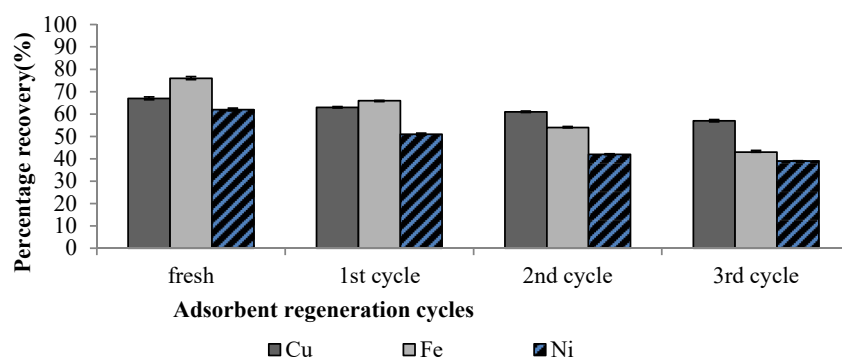### 3.9. Comparison of Cu Fe and Ni ions removal with other studies

The removal of metal ions or contaminants from aqueous solutions through the adsorption process depends on a number of experimental and environmental conditions. The same adsorbent can experience different adsorption capacities for the same contaminant due to such conditions. The adsorbents are selected after determining their

Table 10. Parameters of column kinetic models.

Adsorbent	Heavy metals	Yoon-Nelson model			Thomas model		
		K_{yn} (min^{-1})	T(min)	R^2	K_{TH}(L.min^{-1}.mg^{-1})	q_o (mg.g^{-1})	R^2
MGBW	Copper	-0.0003	23846.33	0.062	0.0000015	8742.93	0.06
	Iron	0.0004	18145	0.07	-0.000002	-6652.61	0.07
	Nickel	-5E-05	-13952	0.002	0.00006	0.002	0.004

Table 11. Performance comparison with other column adsorption studies.

Adsorbents	Contaminant	Initial concentration (mgL^{-1})	Bed height (mm)	Flow rate (mLmin^{-1})	Thomas Adsorption capacity (mgg^{-1})	References
Charcoal from Rubber Wood Sawdust	Pb^{2+}	30	50	15	66794.92	(Biswas and Mishra, 2015)
Coal Fly ash	Cu^{2+}	500	210	10	11.39	Lekgoba et al., 2020
			280		4.26	
Silicate tailings	Cd^{2+}	100	90	5	14.42	Ouyang et al. (2019)
	Pb^{2+}				13.03	
	Cu^{2+}				11.65	
Clay brick waste (MGBW)	Cu^{2+}	200	290	20	8742.93	This study
	Fe^{2+}				-6652.61	
	Ni^{2+}				0.002	

Figure 13. Regeneration trials of clay brick waste adsorbent.
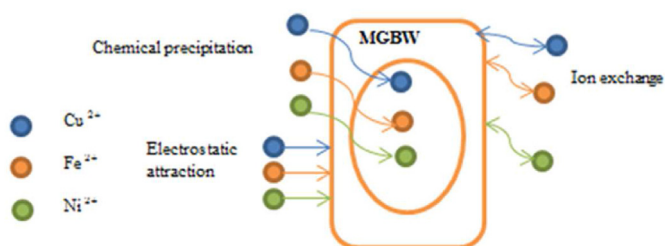
Figure 14. Schematic diagram of adsorption mechanism by MGBW.

adsorption capacities. This is done after conducting a series of experiments that indicate the economic and environmental value of the recommended adsorbent. Different adsorbents were tested for the same metal ions and different results were shown (Table 12). From Table 12, it can be realised that all the studies were conducted using synthetic solutions. In addition, many were conducted through batch mode, with the exception of this study, which used both batch and fixed bed column modes. Investigations at a pilot mode through fixed bed columns mimic field application before field trials. It is also recommended that real wastewater be used during pilot scale because wastewater contains many competing ions and pollutants that might clog the beds, so real field

applications can be predicted. Breakthrough point which may be the national consent of the contaminant or discharge into the environment and saturation points, at which adsorption of the pollutant no longer occurs are determined (Negrea et al., 2021).

3.10. Practical and environmental impact of the study

The reuse of wastewater effluent for agricultural purposes such as horticultural irrigation is gaining momentum in many countries around the world. However, using wastewater effluent for irrigating horticulture projects such as vegetables has health implications that are related to the accumulation of heavy metals in edible plant parts. Therefore, this increases the health risk indices in both children and adults who consume these plants. It is important to reduce such heavy metals from effluents before irrigation. This is also to minimize health risks that may result from the contamination of both groundwater and surface water sources that are abstracted and used for domestic or agricultural purposes. Contamination of water supply sources stresses the limited available water supply sources, resulting in inadequate water supply. The success of this study will fulfil the United Nations Sustainable Development Goal number 3 of 'Good health and well-being and partly goal number 6 of clean water and sanitation.' Adsorption technology through the use of materials that are considered waste is also a green technology for the future as it has no carbon footprint, unlike the use of chemicals that

Table 12. Comparison of this study with other studies.

Metal ion	Adsorbent	Adsorption capacity (mg g^{-1} media)	Experimental conditions	References
Cu	Polish peats	0.48	• Synthetic solution • Batch studies	(Charazi, 2021)
Fe	Polish peats	24.16	• Synthetic solution • Batch studies	(Charazi, 2021)
Ni	Polish peats	0.23	• Synthetic solution • Batch studies	(Charazi, 2021)
Ni	Super magnetic Iron oxide nanoparticles	227.2	• Batch studies • 50–600 mgL^{-1} working solution (synthetic) • At pH and sorbent dose of 0.05 g	(Nithya et al., 2018)
Cu	Bottom ash o expired drugs	13.335	• Batch studies • Synthetic solution • Optimum pH was 6	(Benzaoui et al., 2018)
Cu	Natural Zeolite	0.023	• Batch studies • Synthetic solution	(Belova, 2019)
Fe	Natural Zeolite	0.021	• Synthetic solution	(Belova, 2019)
Ni	Natural Zeolite	0.020	• Synthetic solution	(Belova, 2019)
Cu	Sugarcane activated carbon	2.99	• Batch studies • Synthetic solution	(Tran et al., 2017a, b)
Ni	Sugarcane activated carbon	13.24	• Batch studies • Synthetic solution	(Tran et al., 2017a, b)
Cu	Clay brick waste	• 6.70 (Batch) • 2.22 (Fixed bed)	• Synthetic solution • Batch and fixed-bed column	This study
Ni	Clay brick waste	• 6.20 (Batch) • 0.74 (Fixed bed)	• Synthetic solution • Batch and fixed-bed column	This study
Fe	Clay brick waste	• 7.6 (Batch) 2.23 (Fixed bed)	• Synthetic solution • Batch and fixed-bed column	This study

produce greenhouse gases that contribute to global warming and thereby promoting climate change. The use of adsorption technology for cleaning wastewater promotes goal number 13 of Climate change.

4. Conclusions

The characterisation and potential of Makoro Granite clay brick waste as a heavy metal adsorbent has been investigated. The Quartz and Mullite were the dominant crystalline minerals in the clay brick waste. The dominant elements in fresh clay brick waste were Silicon (Si) followed by Aluminium (Al). In addition, MGBW is an environmentally friendly media as its leachate concentrations were lower than the regulatory levels governing effluent discharge. The TGA findings showed that the chemical bonds in the media were broken at temperatures above 200 °C and lost weight of about 1.353%. Batch studies revealed that Cu^{2+} adsorptive removal onto MGBW at 293K and 303K follows the Langmuir isotherm model while the 313K follows the Freundlich isotherm model. The adsorption of Cu^{2+}, Ni^{2+}, and Fe^{2+} onto media indicated that the chemisorption process took place and that intra-particle diffusion was

not the only rate controlling mechanism. Thermodynamic studies on the adsorption of Cu^{2+}, Ni^{2+}, and Fe^{2+} onto MGBW revealed that the adsorption was non-spontaneous and exothermic process. Fixed – bed column studies showed that divalent copper and iron were highly retained due to their smaller ionic radiuses and high electronegativity compared to nickel. The Yoon-Nelson and Thomas kinetic models describe the adsorption process of copper and nickel better than that of nickel onto MGBW. MGBW showed great regeneration potential with sodium hydroxide solution. In general, MGBW can be used as a heavy metal adsorbent for divalent copper and iron, but not for nickel in polluted water.

Declarations

Author contribution statement

Gobusaone Mokokwe; Moatlhodi Wise Letshwenyo: Conceived and designed the experiments; Performed the experiments; Analyzed and interpreted the data; Contributed reagents, materials, analysis tools or data; Wrote the paper.

Funding statement

Gobusaone Mokokwe was supported by Botswana International University of Science and Technology [S00202].

Data availability statement

Data will be made available on request.

Declaration of interests statement

The authors declare no conflict of interest.

Additional information

No additional information is available for this paper.

Acknowledgements

The authors of this work would like to thank the technical staff at Botswana International University of Science and Technology (BIUST) for the necessary support they provided. We also thank Makoro PTY Ltd for providing us with clay brick waste used as the media in conducting this study.

References

Abdel, O.E., Reiad, N.A., Elshafei, M.M., 2011. A study of the removal characteristics of heavy metals from wastewater by low-cost adsorbents. J. Adv. Res. 2, 297–303.
Adebowale, K.O., Unuabonah, I.E., 2005. Adsorption of some heavy metal ions on sulfate- and phosphate-modified kaolin. Appl. Clay Sci. 29, 145–148.
Ahmad, R., Kumar, R., Haseeb, S., 2012. Adsorption of Cu 2 + from aqueous solution onto iron oxide coated eggshell powder : evaluation of equilibrium , isotherms , kinetics , and regeneration capacity. Arab. J. Chem. 5, 353–359.
Ahmaruzzaman, M., 2011. Industrial wastes as low-cost potential adsorbents for the treatment of wastewater laden with heavy metals. Adv. Colloid Interface Sci. 166, 36–59.
Alanber, M.A., 2011. Thermodynamics Approach in the Adsorption of Heavy Metals, Thermodynamics - Interaction Studies - Solids, Liquids and Gases.
AlSenani, G.M., Al-fawzan, F.F., 2018. Study on Adsorption of Cu and Ba from Aqueous Solutions Using Nanoparticles of Origanum (OR) and Lavandula (LV) 2018. Bioinorganic Chemistry and Applications.
Ali, H., Khan, E., Ilahi, I., 2019. Environmental chemistry and ecotoxicology of hazardous heavy metals: environmental persistence, toxicity, and bioaccumulation. J. Chem. 2019.
Amuda, O., Amoo, I., Ipinmoroti, K., Ajayi, O., 2006. Coagulation/flocculation process in the removal of trace metals present in industrial wastewater. J. Appl. Sci. Environ. Manag. 10, 1–4.

Arias, C.A., Cabello, A., Brix, H., Johansen, N.H., 2003. Removal of indicator bacteria from municipal wastewater in an experimental two-stage vertical flow constructed wetland system. Water Sci. Technol. 48, 35–41.

Babel, S., Kurniawan, T.A., 2003. Low-cost adsorbents for heavy metals uptake from contaminated water: a review. J. Hazard Mater. 97, 219–243.

Bagali, S.S., Gowrishankar, B.S., Roy, A.S., 2017. Optimization , kinetics , and equilibrium studies on the removal of lead (II) from an aqueous solution using Banana pseudostem as an adsorbent. Engineering 3, 409–415.

Bakhtiari, N., Azizian, S., 2015. Adsorption of copper ion from aqueous solution by nanoporous MOF-5 : a kinetic and equilibrium study. J. Mol. Liq. 206, 114–118.

Balouch, A., Kolachi, M., Talpur, F.N., Khan, H., Bhanger, M.I., 2015. Sorption kinetics , isotherm and thermodynamic modeling of defluoridation of ground water using natural adsorbents. Am. J. Anal. Chem. 2013 (4), 221–228.

Belova, T.P., 2019. Heliyon Adsorption of heavy metal ions (Cu 2 þ , Ni 2 þ , Co 2 þ and Fe 2 þ) from aqueous solutions by natural zeolite. Heliyon 5, e02320.

Benzaoui, T., Selatnia, A., Djabali, D., 2018. Adsorption of copper (II) ions from aqueous solution using bottom ash of expired drugs incineration. Adsorpt. Sci. Technol. 36, 114–129.

Bharathi, K.S., Ramesh, S.P.T., 2013. Fixed-bed column studies on biosorption of crystal violet from aqueous solution by Citrullus lanatus rind and Cyperus rotundus. Appl. Water Sci. 3, 673–687.

Biswas, S., Mishra, U., 2015. Continuous fixed-bed column study and adsorption modeling: removal of lead ion from aqueous solution by charcoal originated from chemical carbonization of rubber wood sawdust. J. Chem. 2015.

Bohli, T., 2013. Comparative study of bivalent cationic metals adsorption Pb(II), Cd(II), Ni(II) and Cu(II) on olive stones chemically activated carbon. J. Chem. Eng. Process Technol. 4.

Bouhamed, F., Elouear, Z., Bouzid, J., 2012. Adsorptive removal of copper(II) from aqueous solutions on activated carbon prepared from Tunisian date stones: equilibrium, kinetics and thermodynamics. J. Taiwan Inst. Chem. Eng. 43, 741–749.

Brbooti, M.M., Abid, B.,, Al-shuwaiki, N.M., 2011. Removal of heavy metals using chemicals precipitation. Eng. Technol. J. 29.

Chancey, R.T., Stutzman, P., Juenger, M.C.G., Fowler, D.W., 2010. Comprehensive phase characterization of crystalline and amorphous phases of a Class F fly ash. Cement Concr. Res. 40, 146–156.

Charazĭnśka, S., Lochyński, P., Burszta-Adamiak, E., 2021. Institute Removal of heavy metal ions form acidic electrolyte for stainless steel electropolishing via adsorption using Polish peats. J. Water Process. Eng. 42, 102169.

Charazi, S., 2021. Removal of heavy metal ions form acidic electrolyte for stainless steel electropolishing via adsorption using Polish peats 42. J. Water Proc. Eng. J.

Drizo, A., Frost, C.A., Grace, J., Smith, K.A., 1999. Physico-chemical screening of phosphate-removing substrates for use in constructed wetland systems. Water Res. 33, 3595–3602.

Duan, R., Fedler, C.B., 2021. Adsorptive removal of Pb2+ and Cu2+ from stormwater by using water treatment residuals. Urban Water J. 18, 237–247.

Elshahat, M.F., Shehata, A.M.A., 2013. Adsorption of lead, cadmium and zinc ions from industrial wastewater by using raw clay and broken clay-brick waste. Asian J. Chem. 25, 4284–4288.

Farhan, S.N., Khadom, A.A., 2015. Biosorption of heavy metals from aqueous solutions by Saccharomyces Cerevisiae. Int. J. Ind. Chem. 119–130.

Farooq, U., Kozinski, J.A., Khan, M.A., Athar, M., 2010. Biosorption of heavy metal ions using wheat based biosorbents - a review of the recent literature. Bioresour. Technol. 101, 5043–5053.

Favero, J. da S., Parisotto-Peterle, J., Weiss-Angeli, V., Brandalise, R.N., Gomes, L.B., Bergmann, C.P., dos Santos, V., 2016. Physical and chemical characterization and method for the decontamination of clays for application in cosmetics. Appl. Clay Sci. 124–125, 252–259.

Fierro, V., Torne, V., 2008. Adsorption of phenol onto activated carbons having different textural and surface properties. Microporous Mesoporous Mater. 111, 276–284.

Flouty, R., Estephane, G., 2012. Bioaccumulation and biosorption of copper and lead by a unicellular algae Chlamydomonas reinhardtii in single and binary metal systems: a comparative study. J. Environ. Manag. 111, 106–114.

Foroutan, R., Mohammadi, R., Jamaleddin, S., 2020. Environmental Technology & Innovation Application of nano-silica particles generated from offshore white sandstone for cadmium ions elimination from aqueous media. Environ. Technol. Innovat. 19, 101031.

Gebretsadik, H., Gebrekidan, A., Demlie, L., 2020. Removal of heavy metals from aqueous solutions using Eucalyptus Camaldulensis : an alternate low cost adsorbent Removal of heavy metals from aqueous solutions using Eucalyptus Camaldulensis : an alternate low cost adsorbent. Cogent Chem.

Gill, R., Mahmood, A., Nazir, R., 2013. Biosorption potential and kinetic studies of vegetable waste mixture for the removal of Nickel(II). J. Mater. Cycles Waste Manag. 15, 115–121.

Haile, T.M., Fuerhacker, M., 2018. Simultaneous adsorption of heavy metals from roadway stormwater runoff using different filter media in column studies. Water (Switzerland) 10, 1–18.

Hajira, T., Atika, S., Muhammad, S., 2018. Synthesis of kaolin loaded Ag and Ni nanocomposites and their applicability for the removal of malachite green oxalate dye. Iran. J. Chem. Chem. Eng. 37, 11–22.

Hemalatha, P.V., Rao, V.V.P., 2014. Adsorption batch studies on calcined brick powder in removing chromium and nickel ions. Int. J. Adv. Res. Comput. Sci. 1, 14–21.

Hu, J., Chen, G., Lo, I.M.C., 2005. Removal and recovery of Cr(VI) from wastewater by maghemite nanoparticles. Water Res. 39, 4528–4536.

Iloms, E., Ololade, O.O., Ogola, H.J.O., 2020. Investigating industrial E ffluent impact on municipal wastewater treatment plant in vaal , South Africa. Int. J. Environ. Res. Publ. Health 1–18.

Janbuala, S., Wasanapiarnpong, T., 2015. Effect of rice husk and rice husk ash on properties of lightweight clay bricks. Key Eng. Mater. 659, 74–79.

Jellali, S., Wahab, M.A., Hassine, R. Ben, Hamzaoui, A.H., Bousselmi, L., 2011. Adsorption characteristics of phosphorus from aqueous solutions onto phosphate mine wastes. Chem. Eng. J. 169, 157–165.

Jia, L., Shukla, S.S., Dorris, K.L., Shukla, A., Margrave, J.L., 2003. Adsorption of chromium from aqueous solutions by maple sawdust. J. Hazard Mater. 100, 53–63.

Jozanikohan, G., Nosrati, M., 2022. The Fourier transform infrared spectroscopy (FTIR) analysis for the clay mineralogy studies in a clastic reservoir. J. Pet. Explor. Prod. Technol.

Kapur, M., Mondal, M.K., 2014. Competitive sorption of Cu(II) and Ni(II) ions from aqueous solutions: kinetics, thermodynamics and desorption studies. J. Taiwan Inst. Chem. Eng. 45, 1803–1813.

Khulbe, K.C., Matsuura, T., 2018. Removal of heavy metals and pollutants by membrane adsorption techniques. Appl. Water Sci. 8, 1–30.

Kong, L., Wang, M., Chao, J., 2019. Removal of Cu 2 + and Ni 2 + from wastewater by using modified alkali-leaching residual wire sludge as low cost adsorbent. Water Air Soil Pollut. 230 (2019), 65.

Ku, Y., Jung, I.L., 2001. Photocatalytic reduction of Cr(VI) in aqueous solutions by UV irradiation with the presence of titanium dioxide. Water Res. 35, 135–142.

Lai, Y., Thirumavalavan, M., Lee, J., 2010. Effective adsorption of heavy metal ions (Cu , Pb , Zn) from aqueous solution by immobilization of adsorbents on Ca-alginate beads 2248. Toxicol. Environ. Chem. 92 (4), 697–705.

Lekgoba, T., Ntuli, F., Falayi, T., 2020. Application of coal fly ash for treatment of wastewater containing a binary mixture of copper and nickel. J. Water Proc. Eng. 101822.

Letina, D., Letshwenyo, W.M., 2018. Investigating waste rock, tailings, slag and coal ash clinker as adsorbents for heavy metals: batch and column studies. Phys. Chem. Earth 105, 184–190.

Letshwenyo, M., Mokokwe, G., 2020. Accumulation of heavy metals and bacteriological indicators in spinach irrigated with further treated secondary wastewater. Heliyon 6, e05241.

Letshwenyo, M.W., Mokokwe, G., 2021. Phosphorus and sulphates removal from wastewater using copper smelter slag washed with acid. SN Appl. Sci. 3.

Liu, M., Almatra, E., Zhang, Y., Xu, P., Song, B., Zhou, C., Zeng, G., Zhu, Y., 2022. A critical review of biochar-based materials for the remediation of heavy metal contaminated environment : applications and practical evaluations. Sci. Total Environ. 806.

MacÍas-Quiroga, I.F., Giraldo-Gómez, G.I., Sanabria-González, N.R., 2018. Characterization of Colombian clay and its potential use as adsorbent. Sci. World J. 2018, 15–17.

Malkoc, E., Nuhoglu, Y., 2006. Removal of Ni(II) ions from aqueous solutions using waste of tea factory: adsorption on a fixed-bed column. J. Hazard Mater. 135, 328–336.

Manjuladevi, M., Anitha, R., Manonmani, S., 2018. Kinetic study on adsorption of Cr(VI), Ni(II), Cd(II) and Pb(II) ions from aqueous solutions using activated carbon prepared from Cucumis melo peel. Appl. Water Sci. 8, 1–8.

Martins, B., Vilar, R.J.E., Boaventura, R.A.R., 2014. Kinetic modelling of cadmium and lead removal by aquatic mosses. Braz. J. Chem. Eng. 31, 229–242.

Mishra, S.R., Chandra, R., Kaila, A.,J., Darshi, B.,S., 2017. Kinetics and isotherm studies for the adsorption of metal ions onto two soil types. Environ. Technol. Innovat. 7, 87–101.

Mushtaq, M., Tan, I.M., Ismail, L., Nadeem, M., Sagir, M., Azam, R., Hashmet, R., 2014. Influence of PZC (point of zero charge) on the static adsorption of anionic surfactants on a Malaysian sandstone. J. Dispersion Sci. Technol. 35, 343–349.

Negrea, A., Mihailescu, M., Mosoarca, G., Ciopec, M., 2021. Estimation on fixed-bed column parameters of breakthrough behaviors for gold recovery by adsorption onto modified/functionalized amberlite XAD7. n.d. Int. J. Environ. Res. Publ. Health 18, 13339.

Neris, J.B., Luzardo, F.H.M., da Silva, E.G.P., Velasco, F.G., 2019. Evaluation of adsorption processes of metal ions in multi-element aqueous systems by lignocellulosic adsorbents applying different isotherms: a critical review. Chem. Eng. J. 357, 404–420.

Nie, R., 2021. Removal of multiple metal ions from wastewater by a multifunctional metal-organic- framework based trap. Water Sci. Technol. 84 (7), 1594–1607.

Nithya, K., Sathish, A., Kumar, P.S., Ramachandran, T., 2018. Journal of Industrial and Engineering Chemistry Fast kinetics and high adsorption capacity of green extract capped superparamagnetic iron oxide nanoparticles for the adsorption of Ni (II) ions. J. Ind. Eng. Chem. 59, 230–241.

Njoku, P., Bennard, O., Akudinobi, B., 2020. Potential health risk and levels of heavy metals in water resources of lead – zinc mining communities of Abakaliki , southeast Nigeria. Appl. Water Sci. 10, 1–23.

Nosrati, A., Addai-mensah, J., Skinner, W., 2009. pH-mediated interfacial chemistry and particle interactions in aqueous muscovite dispersions. Chem. Eng. J. 152, 406–414.

Omopariola, A.O., Adeniyi, F.I., 2021. Environmental Sciences and Ecology (ESECR) Evaluation of the Physico-Chemical Characteristics and Heavy Metal Contents of Shasha River, Southwestern Nigeria. ESECR 2 (2).

Osińska, M., 2017. Removal of lead(II), copper(II), cobalt(II) and nickel(II) ions from aqueous solutions using carbon gels. J. Sol. Gel Sci. Technol. 81, 678–692.

Ouyang, D., Zhuo, Y., Hu, L., Zeng, Q., Hu, Y., He, Z., 2019. Research on the adsorption behavior of heavy metal ions by porous material prepared with silicate tailings. Minerals 9, 1–16.

Pan, J., Gao, B., Wang, S., Guo, K., Xu, X., Yue, Q., 2020. Science of the Total Environment Waste-to-resources : green preparation of magnetic biogas residues-based biochar for effective heavy metal removals. Sci. Total Environ. 737, 140283.

Rahman, S., Sathasivam, K.V., 2015. Heavy metal adsorption onto kappaphycus sp . from aqueous solutions : the use of error functions for validation of isotherm and kinetics models. BioMed Res. Int. 2015.

Rajeshkannan, R., Rajasimman, M., Rajamohan, N., 2013. Proučavanje uklanjanje boja novim sorbentom u koloni sa pakovanim slojem. Chem. Ind. Chem. Eng. Q. 19, 461–470.

Ramakrishnaiah, C.R., Prathima, B., 2016. Hexavalent chromium removal by chemical precipitation method : a comparative study. Int. J. Environ. Res. Dev. 1, 41–49.

Rüscher, C.H., Lohaus, L., Jirasit, F., 2022. Alkali-Activated Slags and CEMI/CEMIII Pastes : Implications for Next Generation Concretes. Gels.

Sabela, M.I., Kunene, K., Kanchi, S., Xhakaza, N.M., Bathinapatla, A., Mdluli, P., Sharma, D., Bisetty, K., 2019. Removal of copper (II) from wastewater using green vegetable waste derived activated carbon: an approach to equilibrium and kinetic study. Arab. J. Chem. 12, 4331–4339.

Sarma, G.K., Sen Gupta, S., Bhattacharyya, K.G., 2019. Nanomaterials as versatile adsorbents for heavy metal ions in water: a review. Environ. Sci. Pollut. Res. 26, 6245–6278.

Sharma, A., Bhattacharyya, K.G., 2005. Adsorption of chromium (VI) on azadirachta indica (neem) leaf powder. Adsorption 10, 327–338.

Singh, S.K., Mehta, D., Sehgal, D., 2015. Fixed bed column study and adsorption modelling on the adsorption of malachite green dye from wastewater using acid activated sawdust evaluation of tigris river by water quality index analysis using C++ program view project status of health and sanitation. Artic. Int. J. Adv. Res. 4, 968.

Siong, W., Ying, J., Kumar, P.S., Mubashir, M., Majeed, Z., Banat, F., Ho, S., Loke, P., 2021. A review on conventional and novel materials towards heavy metal adsorption in wastewater treatment application. J. Clean. Prod. 296, 126589.

Son, E., Poo, K., Chang, J., Chae, K., 2018. Science of the Total Environment Heavy metal removal from aqueous solutions using engineered magnetic biochars derived from waste marine macro-algal biomass. Sci. Total Environ. 615, 161–168.

Tan, J.J., Huang, Y., Wu, Z.Q., Chen, X., 2017. Ion exchange resin on treatment of copper and nickel wastewater. IOP Conf. Ser. Earth Environ. Sci. 94.

Thaçi, B.S., Gashi, S.T., 2019. Reverse osmosis removal of heavy metals from wastewater effluents using biowaste materials pretreatment. Pol. J. Environ. Stud. 28, 337–341.

Tran, H.N., You, S.J., Hosseini-Bandegharaei, A., Chao, H.P., 2017a. Mistakes and inconsistencies regarding adsorption of contaminants from aqueous solutions: a critical review. Water Res. 120, 88–116.

Tran, T., Van, Thi, Q., Bui, P., 2017b. A comparative study on the removal efficiency of metal using sugarcane bagasse- derived ZnCl 2 -activated carbon by the response surface methodology. Sci. Technol. 35 (1–2), 72–85.

Trgo, M., Medvidović, N.V., Perić, J., 2011. Application of mathematical empirical models to dynamic removal of lead on natural zeolite clinoptilolite in a fixed bed column. Indian J. Chem. Technol. 18, 123–131.

US EPA, 2002. Standard Operating Procedures Soil pH Determination 1–6.

Usman, K., Khan, S., Ghulam, S., Khan, M.U., Khan, M.A., Khalil, S.K., 2012. Sewage sludge: an important biological resource for sustainable agriculture and its environmental implications. Am. J. Plant Sci. 3 (12), 1708–1721.

Vareda, J.P., Valente, A.J.M., Durães, L., 2019. Assessment of heavy metal pollution from anthropogenic activities and remediation strategies : a review. J. Environ. Manag. 246, 101–118.

Viegas, R.M.C., Campinas, M., Costa, H., Rosa, M.J., 2014. How do the HSDM and Boyd's model compare for estimating intraparticle diffusion coefficients in adsorption processes. Adsorption 20, 737–746.

Visa, M., 2016. Synthesis and characterization of new zeolite materials obtained from fly ash for heavy metals removal in advanced wastewater treatment. Powder Technol. 294, 338–347.

Wang, X., Cui, Y., Peng, Q., Fan, C., Zhang, Z., Zhang, X., 2020. Removal of Cd (II) and Cu (II) from aqueous solution by Na + - modified Pisha sandstone. J. Chem.

Wierzba, S., 2017. Biosorption of nickel (II) and zinc (II) from aqueous solutions by the biomass of yeast Yarrowia lipolytica. Pol. J. Chem. Technol. 19, 1–10.

Wołowiec, M., Komorowska-kaufman, M., Pruss, A., Rzepa, G., Bajda, T., 2019. Removal of heavy metals and metalloids from water using drinking water treatment residuals as adsorbents : a review. Minerals 1–17. https://www.mdpi.com/2075-163X/9/8/487#.

Xu, L., Zheng, X., Cui, H., Zhu, Z., Liang, J., Zhou, J., 2017. Equilibrium , kinetic , and thermodynamic studies on the adsorption of cadmium from aqueous solution by modified biomass ash. Bioinorgan. Chem. Appl. 2017.

Younas, F., Mustafa, A., Farooqi, Z.U.R., Wang, X., Younas, S., Mohy-Ud-din, W., Hameed, M.A., Abrar, M.M., Maitlo, A.A., Noreen, S., Hussain, M.M., 2021. Current and emerging adsorbent technologies for wastewater treatment: trends, limitations, and environmental implications. Water (Switzerland) 13, 1–25.

Zhang, X., Wang, X., 2015. Adsorption and desorption of Nickel(II) ions from aqueous solution by a lignocellulose/montmorillonite nanocomposite. PLoS One 10, 1–21.

Zyoud, A.H., Asaad, S., Zyoud, Samer H., Zyoud, Shaher H., Helal, M.H., Qamhieh, N., Hajamohideen, A.R., Hilal, H.S., 2020. Raw clay supported ZnO nanoparticles in photodegradation of 2-chlorophenol under direct solar radiations. J. Environ. Chem. Eng. 8, 104227.